Langmuir

ARTICLE

pubs.acs.org/Langmuir

Looped Structure of Flowerlike Micelles Revealed by ^{1}H NMR Relaxometry and Light Scattering

Albert J. de Graaf,[†,⊥] Kristel W. M. Boere,[†,⊥] Johan Kemmink,[‡] Remco G. Fokkink,[∥] Cornelus F. van Nostrum,[†] Dirk T. S. Rijkers,[‡] Jasper van der Gucht,[∥] Hans Wienk,[§] Marc Baldus,[§] Enrico Mastrobattista,[†] Tina Vermonden,[†] and Wim E. Hennink*[,†]

[†]Utrecht Institute for Pharmaceutical Sciences, Pharmaceutics, and [‡]Medicinal Chemistry & Chemical Biology, Utrecht University, P.O. Box 80.082, 3508TB Utrecht, The Netherlands

[§]Bijvoet Center for Biomolecular Research, NMR Spectroscopy Research Group, Utrecht University, Padualaan 8, 3584CH Utrecht, The Netherlands

[∥]Laboratory of Physical Chemistry and Colloid Science, Wageningen University, P.O. Box 8038, 6700EK Wageningen, The Netherlands

Supporting Information

ABSTRACT: We present experimental proof that so-called "flowerlike micelles" exist and that they have some distinctly different properties compared to their "starlike" counterparts. Amphiphilic AB diblock and BAB triblock copolymers consisting of poly(ethylene glycol) (PEG) as hydrophilic A block and thermosensitive poly(*N*-isopropylacrylamide) (pNIPAm) B block(s) were synthesized via atom transfer radical polymerization (ATRP). In aqueous solutions, both block copolymer types form micelles above the cloud point of pNIPAm. Static and dynamic light scattering measurements in combination with NMR relaxation experiments proved the existence of flowerlike micelles based on $pNIPAm_{16kDa}$-PEG_{4kDa}-$pNIPAm_{16kDa}$ which had a smaller radius and lower mass and aggregation number than starlike micelles based on $mPEG_{2kDa}$-$pNIPAm_{16kDa}$. Furthermore, the PEG surface density was much lower for the flowerlike micelles, which we attribute to the looped configuration of the hydrophilic PEG block. ^{1}H NMR relaxation measurements showed biphasic T_2 relaxation for PEG, indicating rigid PEG segments close to the micelle core and more flexible distal segments. Even the flexible distal segments were shown to have a lower mobility in the flowerlike micelles compared to the starlike micelles, indicating strain due to loop formation. Taken together, it is demonstrated that self-assemblies of BAB triblock copolymers have their hydrophilic block in a looped conformation and thus indeed adopt a flowerlike conformation.

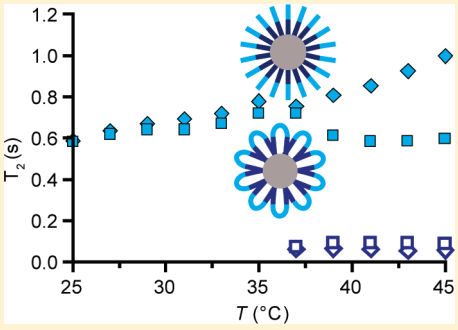

INTRODUCTION

Polymeric micelles are widely studied as delivery vehicles for hydrophobic, low molecular weight drugs.[1−8] Two important features are their generally low critical micelle concentration (CMC) as compared to low molecular weight amphiphiles and their small size (several tens of nanometers) which renders them suitable for passive targeting exploiting the enhanced permeability and retention effect.[9,10] Furthermore, the highly hydrated shell of the micelles can shield them from recognition and uptake by cells of the immune system. Poly(ethylene glycol) (PEG), which is well-known for these stealthlike properties, is therefore often used to form the hydrophilic corona.[11] Polymeric micelles, with a hydrophobic core and a hydrophilic shell, are obtained by dispersing amphiphilic AB block copolymers in water.[1−8] BAB triblock copolymers with a hydrophilic midblock flanked by two hydrophobic blocks have been hypothesized to self-assemble into so-called "flowerlike micelles".[12−16] For drug delivery purposes, these flowerlike micelles might have several advantages over their starlike counterparts, like a potentially lower CMC and higher kinetic stability.[17−19] It must be noted that, although a flowerlike structure is intuitively logical, there is at present only indirect evidence to support its existence. It has been shown that theoretically flowerlike micelles can exist, if the entropic penalty of looping the hydrophilic blocks is smaller than the free energy decrease of micellization.[20−22] Small-angle X-ray and neutron scattering data on some BAB block copolymers could be fitted to a core−shell model under some assumptions.[23,24] On the other hand, other authors claim based on simulations that self-assemblies of BAB block copolymers may not be "real" micelles having a well-separated core and corona.[25,26]

The aim of the present study is to indisputably prove the existence of flowerlike micelles by proving that their hydrophilic blocks are in a looped conformation. Therefore, the size, aggregation number, and surface graft density of flowerlike and starlike micelles are compared. Furthermore, the segmental mobility of the hydrophilic PEG blocks in starlike and flowerlike

Received: May 25, 2011
Revised: July 14, 2011
Published: July 14, 2011

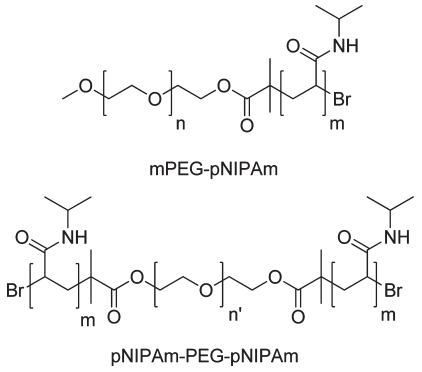

Figure 1. Structure of mPEG-pNIPAm and pNIPAm-PEG-pNIPAm. $n = 44$, $n' \in \{44, 90, 135\}$, $m = 140$.

micelles is studied by ^{1}H NMR relaxometry as a function of architecture, block length, and temperature.

Model System. As model system, we chose block copolymers of AB and BAB architecture consisting of a poly(ethylene glycol) (PEG) A block and thermosensitive poly(*N*-isopropylacrylamide) (pNIPAm) B block(s) (Figure 1). Above the cloud point (CP) of the thermosensitive blocks (~32 °C for pNIPAm homopolymer in water[27]), these AB and BAB polymers form micelles. For a fair comparison between diblock and triblock copolymers, we compared $pNIPAm_{16kDa}$-PEG_{4kDa}-$pNIPAm_{16kDa}$ to $mPEG_{2kDa}$-$pNIPAm_{16kDa}$ so that the triblock copolymer can be considered as a double diblock copolymer. To study the influence of the PEG length on the loop structure, triblock copolymers with either a shorter (2 kDa) or longer (6 kDa) PEG block were prepared as well. The polymers were prepared by atom transfer radical polymerization (ATRP) of NIPAm onto (m)PEG macroinitiators.

EXPERIMENTAL SECTION

Chemicals. *N*-Isopropylacrylamide (NIPAm; Aldrich, 97%) was recrystallized twice from a mixture of *n*-hexane and toluene (v/v = 1:1). Poly(ethylene glycol) (PEG) with molar masses of 2000, 4000, and 6000 Da and poly(ethylene glycol) monomethyl ether (mPEG) with molar mass of 2000 Da were purchased from Merck and dehydrated prior to use by coevaporation of water with toluene at 84−110 °C. Tris(2-dimethylaminoethyl)amine (Me_6TREN) was prepared according to reported procedures.[28] 2-Bromoisobutyryl bromide (Aldrich), copper bromide, and copper dibromide (Acros) were used as received.

Synthesis of (m)PEG Macroinitiators. Dehydrated (m)PEG (5.0 g, different molecular weights) was dissolved in 100 mL of THF dried on molecular sieves and degassed by flushing with nitrogen. Subsequently, 1.1 equiv of triethylamine (to −OH groups) and 1.1 equiv of bromoisobutyryl bromide (to −OH groups) were added. The mixture was allowed to react overnight at room temperature, after which the bromide salt was filtrated off. The filtrate was concentrated and again dissolved in dichloromethane. The crude product was precipitated in cold diethyl ether and filtrated. A white product was formed with a yield of ~80%. ^{1}H NMR (300 MHz, $CDCl_3$): mPEG macroinitiator, δ 4.3 ppm (t, 2H, OCH_2), δ 3.85 ppm (t, 2H, OCH_2), δ 3.65 ppm (t, 4nH, OCH_2), δ 3.35 ppm (t, 2H, OCH_2), δ 3.30 ppm (s, 3H, OCH_3), δ 1.85 ppm (s, 6H, CCH_3). PEG macroinitiator, δ 4.3 ppm (t, 4H, OCH_2), δ 3.85 ppm (t, 4H, OCH_2), δ 3.65 ppm (t, 4nH, OCH_2), δ 3.35 ppm (t, 4H, OCH_2), δ 1.85 ppm (s, 12H,CCH_3). Also, ^{1}H NMR spectra after addition of two droplets of trichloroacetyl isocyanate (TAIC) were taken to determine the degree of substitution. These spectra confirmed that the (m)PEG was >95% functionalized.

Synthesis of mPEG-pNIPAm and pNIPAm-PEG-pNIPAm Copolymers. 200 mg of (m)PEG macroinitiator, 18.1 mg of CuBr, and 18.8 mg of $CuBr_2$ and the correct amount of NIPAm for the aimed block length were dissolved in 10 mL of H_2O and 2.5 mL of acetonitrile. A stirring bar was introduced; the solution was degassed by flushing with N_2 for half an hour and placed in an ice bath for another 15 min. The reaction was started by adding 0.5 mL of 0.42 M Me_6TREN solution, which turned the mixture immediately blue. Periodically, 20 μL samples were taken, diluted in air-saturated D_2O, and analyzed by ^{1}H NMR to determine the NIPAm conversion. When the conversion had reached 95%, the reaction was quenched by flushing with air for 1 min. The crude product was dialyzed against water overnight and subsequently freeze-dried. The yield was ~90%.

The polymers were characterized by ^{1}H NMR with a Gemini 300 MHz spectrometer (Varian Associates Inc., NMR Instruments, Palo Alto, CA) and GPC. GPC was done using 2 PLgel 3 μm Mixed-D columns (Polymer Laboratories). The eluent was DMF containing 10 mM LiCl, the elution rate was set to 0.7 mL/min, and the temperature to 40 °C. Detection was done using a Viscotek TDA triple detector array. dn/dc was determined by the software based on the RI detector signal and the amount of injected polymer.

Formation of Micelles. It has been shown that the size and polydispersity of thermosensitive micelles decrease with increasing the speed at which the cloud point (CP) is passed.[29] Therefore, micelles were formed by adding 100 μL of an aqueous polymer solution (1 mg/mL, at room temperature) to 900 μL water at 50 °C and equilibrating for 5 min. Using this "heat-shock" procedure, micelles having a small radius and low polydispersity were formed.

Determination of the Cloud Point (CP). The CP's were determined by differential scanning calorimetry using a TA systems DSC-Q1000. The polymers were dissolved in a concentration of 3.3% in deionized water at room temperature. Samples of 10 μL were pipetted into aluminum pans which were subsequently hermetically closed, and the temperature was increased from 25 to 50 °C with 5 °C/min. The cloud point was taken as the onset point of the endotherm peak.

Determination of the Critical Micelle Concentration (CMC). The CMC's of the block copolymers were measured using pyrene as a fluorescent probe.[30] The different block copolymers were dissolved in water in concentrations ranging from 1 μg/mL to 1 mg/mL. 15 μL of pyrene dissolved in acetone (1.8×10^{-4} M) was added to 4.5 mL of polymer solution. The micelles were formed by rapidly heating the solutions to 45 °C. After incubation for 16 h at this temperature, pyrene fluorescence was measured using a Horiba Fluorolog fluorometer. Excitation spectra were recorded at 45 °C from 300 to 360 nm with the emission wavelength at 390 nm. The ratio I_{338}/I_{333} was plotted against the logarithmic polymer concentration to determine the CMC.

Dynamic Light Scattering (DLS). DLS measurements were performed on a Malvern CGS-3 goniometer (Malvern Ltd., Malvern, U.K.) coupled to an LSE-5003 autocorrelator, a thermostated water bath, a He−Ne laser (25 mW, 633 nm, equipped with a model 2500 remote interface controller, Uniphase), and a computer with DLS software (PCS, version 3.15, Malvern). The measurement temperature was 40 °C, and the measurement angle was 90°. The solvent viscosity was corrected for the temperature by the software.

Static Light Scattering (SLS). Static light scattering measurements were performed to determine the weight-average molecular weight of the micelles and the radius of gyration. Measurements were performed on an ALV 7002 correlator, ALV-SP/86 goniometer, RFIB263 KF photomultiplier detector with ALV 200 μm pinhole detection system and a Cobolt Samba-300 DPSS laser. The wavelength was set to 532 nm and the power to 300 mW, and the temperature was controlled by a Haake Phoenix II-C30P thermostatic bath. The second-order correlation function, $G_2(t)$, and total averaged scattered intensity were recorded 5 times per angle, for 21 angles, from 20° to 120° in

Table 1. Characteristics of mPEG-pNIPAm and pNIPAm-PEG-pNIPAm Copolymers

	$M_{n,th}$ (kDa)[a]	M_n (kDa)[b]	M_w/M_n[c]	CP (°C)[d]	CMC (mg/mL)[e]	R_h (nm)[f]	PDI[f]
$mPEG_{2000}$-$pNIPAm_{16000}$	18.0	18.2	1.03	36.2 ± 0.1	0.03 ± 0.01	35 ± 2	0.04 ± 0.02
$pNIPAm_{16000}$-PEG_{2000}-$pNIPAm_{16000}$	34.0	34.0	1.09	35.7 ± 0.1	0.02 ± 0.01	30 ± 2	0.05 ± 0.01
$pNIPAm_{16000}$-PEG_{4000}-$pNIPAm_{16000}$	36.0	35.7	1.14	36.7 ± 0.1	0.02 ± 0.01	27 ± 2	0.08 ± 0.03
$pNIPAm_{16000}$-PEG_{6000}-$pNIPAm_{16000}$	38.0	36.6	1.15	36.6 ± 0.1	0.03 ± 0.01	24 ± 2	0.06 ± 0.05

[a] Theoretical M_n. based on monomer/initiator ratio. [b] Determined by NMR. [c] Determined by GPC. [d] Determined by differential scanning calorimetry. [e] Determined from pyrene excitation spectra. [f] Measured with DLS at 0.1 mg/mL concentration, 40 °C and 90° scattering angle. Reported values are averages ± SD of three measurements.

increments of 5° to evaluate the angular dependence of the diffusion coefficient, D, and the excess Rayleigh ratio, R. This procedure was performed for five different concentrations near the CMC of the block copolymer. The SLS experiments were analyzed by a Zimm approximation (more details in the Supporting Information).

^{1}H NMR Relaxation Measurements. For the relaxation measurements, micelles were formed using the above-mentioned heat-shock procedure as described under Formation of Micelles, with the exception that deuterium oxide was used as the solvent. T_1 and T_2 relaxation times were measured from 45 to 25 °C on a Bruker 500 MHz spectrometer. At each temperature, a delay of 10 min allowed the stabilization of the sample temperature. The spin−lattice relaxation time, T_1, was studied by the inversion recovery method. The spin spin relaxation time, T_2, was studied by the Carr−Purcell−Meiboom−Gill pulse sequence. Relaxation times were obtained by nonlinear least-squares fitting of a monoexponential function except that T_2 values above the CP were determined by fitting a biexponential function.

RESULTS AND DISCUSSION

General Properties of Polymers. All polymerizations were well controlled (see Figure S1, Supporting Information). Table 1 summarizes the properties of the synthesized copolymers and their micelles. The molecular weights of the polymers agreed very well with the monomer/initiator feed ratio and their polydispersity, as expected for a living polymerization, was low.

The CP's were higher than the well-known value of 32 °C for homopolymers of NIPAm. This is known to be due to the relatively short pNIPAm length of 16 kDa allowing the hydrophilic PEG to have a significant effect on the CP.[31,32] The CMC of the different polymers was 0.02−0.03 mg/mL (Table 1), consistent with literature on mPEG-pNIPAm.[33] No significant differences in CMC were found between the diblock and triblock copolymers. This indicates that the expected effect of lowering the CMC by having two hydrophobic blocks in the BAB polymer is counteracted by the entropic penalty from the looped configuration of the PEG block. This unfavorable entropy contribution of the bending hydrophilic middle block was also reported in other studies, where triblock copolymers had even higher CMC's than corresponding diblock copolymers.[34,35] Dynamic light scattering measurements showed that micelles of the triblock pNIPAm-PEG-pNIPAm polymers had a hydrodynamic radius (R_h) of 24−30 nm; the micelles of the diblock mPEG-pNIPAm revealed a significantly larger R_h of 35 nm (Table 1). The micelles remained stable for at least 24 h at 40 °C in water. The micelles were rather monodisperse as indicated by a polydispersity index (PDI) < 0.1. Interestingly, the size of the flowerlike micelles decreases with increasing PEG length. We hypothesize that this is caused by an increased PEG "headgroup" area that causes less polymer chains to fit into one micelle.

Static Light Scattering. Static light scattering experiments were performed to investigate what effect the looped PEG conformation and the PEG length have on the surface area per PEG chain and aggregation number for the different micelles (Table 2). First of all, the R_g/R_h ratios (0.78−0.93) are within experimental errors similar for all micelles and are slightly higher than the value of $(3/5)^{1/2}$ = 0.775 that can be calculated for a hard sphere.[36] This is compatible with micelles of which the corona is highly hydrated but still constitutes a significant fraction of the micelle's mass. When comparing the diblock $mPEG_{2kDa}$-$pNIPAm_{16kDa}$ with triblock $pNIPAm_{16kDa}$-PEG_{4kDa}-$pNIPAm_{16kDa}$, a 3.3 times lower aggregation number (N_{agg}) and 2.6 times higher surface area per PEG chain (S/N_{agg}) were found for the flowerlike micelles compared to the starlike micelles. In both cases, a factor of only 2 would be expected if the triblock would simply behave as a "double diblock". These findings can be explained by a looped conformation of the PEG chains in the flowerlike micelles, which forces them into a more mushroom- than brushlike conformation and therefore to occupy a larger surface area. This in turn causes less pNIPAm chains to fit in the core of the micelle, as also represented by the lower overall density of the micelles composed of triblock copolymers as compared to those of diblocks. Table 2 also shows that with increasing PEG block length the surface area per PEG chain in the flowerlike micelles increases and consequently their aggregation number decreases. Clearly, upon increasing the PEG molecular weight the PEG "headgroup" size thus increases not (only) in the radial direction but also in the tangential direction.

^{1}H NMR Relaxometry. ^{1}H NMR spectra were recorded for both $mPEG_{2kDa}$-$pNIPAm_{16kDa}$ and $pNIPAm_{16kDa}$-PEG_{4kDa}-$pNIPAm_{16kDa}$ at temperatures below and above the CP (Figure S2, Supporting Information). For both polymers, above the CP a clear loss of pNIPAm signals is visible while the integral of the PEG signal remains constant. This indicates the formation of micelles with a dense core and hydrated shell above the CP.[37] The PEG signal does, however, broaden at the base above the CP (see below). The micelles were further studied by ^{1}H NMR relaxation measurements, which provide a good measure of polymer chain flexibility.[38] Specifically, it has repeatedly been shown that restricting mobility of PEG chains leads to shorter T_2 times.[39,40] To study the relaxation behavior, ^{1}H NMR T_1 and T_2 relaxation measurements were performed at temperatures between 25 and 40 °C. All T_1 relaxation times were obtained from monoexponential fits (Figure S3, Supporting Information). The T_2 decay curves could also be well fitted by monoexponential decays below the CP (R^2 > 0.99). On the other hand, close inspection of the T_2 decay curves above the CP shows a deviation from monoexponential decay (Figure 2a), leading to low R^2 values for monoexponential fits. Instead, above the CP the decay of the PEG peak integral I with relaxation delay τ could be well

dx.doi.org/10.1021/la2019605 |Langmuir 2011, 27, 9843–9848

Table 2. Characteristics of mPEG-pNIPAm and pNIPAm-PEG-pNIPAm Polymeric Micelles Measured by Simultaneous SLS and DLS

	R_g (nm)[a]	R_{hyd}[b] (nm)	R_g/R_h	$M_{w(mic)}$[b] (10^6 Da)	$\rho_{(mic)}$[c] (g/cm^3)	N_{agg}[d]	S/N_{agg}[e] (nm^2)
$mPEG_{2K}$-$pNIPAm_{16K}$	38 ± 3	40 ± 3	0.95 ± 0.09	80 ± 15	0.38 ± 0.05	4426 ± 818	4.8 ± 0.9
$pNIPAm_{16K}$-PEG_{2K}-$pNIPAm_{16K}$	28 ± 1	36 ± 3	0.78 ± 0.08	59 ± 15	0.51 ± 0.04	1745 ± 432	9.4 ± 0.8
$pNIPAm_{16K}$-PEG_{4K}-$pNIPAm_{16K}$	28 ± 5	34 ± 3	0.83 ± 0.11	28 ± 5	0.30 ± 0.07	1324 ± 535	12.5 ± 4.2
$pNIPAm_{16K}$-PEG_{6K}-$pNIPAm_{16K}$	28 ± 2	31 ± 4	0.90 ± 0.04	19 ± 7	0.25 ± 0.02	500 ± 176	25.3 ± 2.6

[a] Radius of gyration, extrapolated to zero concentration. [b] Extrapolated to zero concentration and zero scattering angle. [c] Density of the micelles. [d] Aggregation number of the micelles. [e] Surface area per PEG chain. All measurements were performed at 40 °C. Reported values are averages ± SD from three measurements.

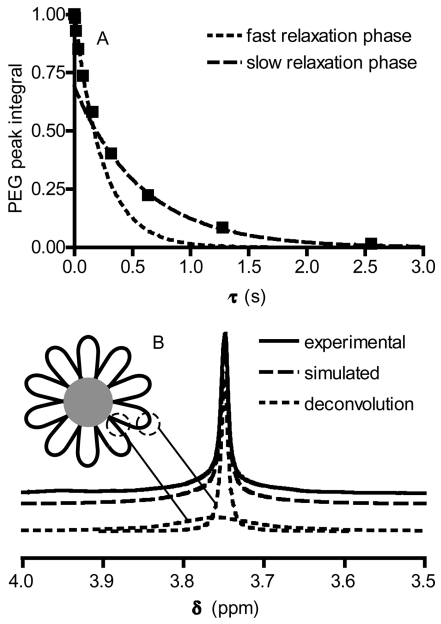

Figure 2. T_2 relaxation behavior of the PEG peak of $pNIPAm_{16000}$-PEG_{4000}-$pNIPAm_{16000}$ at 41 °C: (A) T_2 decay curve showing biphasic relaxation and (B) deconvolution of the PEG peak into a broad (fast relaxing) and narrow (slowly relaxing) component.

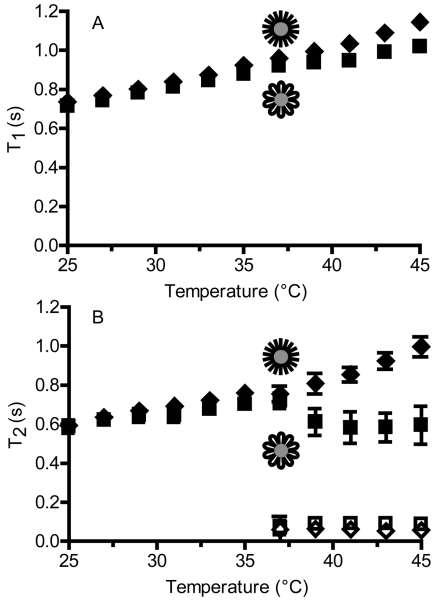

Figure 3. T_1 (A) and T_2 (B) relaxation times of protons in PEG for diblock $mPEG_{2kDa}$-$pNIPAm_{16kDa}$ and triblock $pNIPAm_{16kDa}$-PEG_{4kDa}-$pNIPAm_{16kDa}$ as a function of temperature. Diamonds: diblock; squares: triblock. Error bars indicate the 95% confidence interval.

fitted ($R^2 > 0.99$) by the biexponential equation

$$I_\tau = (f_{fast}e^{-\tau/T_{2fast}} + f_{slow}e^{-\tau/T_{2slow}})I_0 \quad (1)$$

yielding a fast (T_{2fast}) and slow (T_{2slow}) relaxation time. f_{fast} and f_{slow} represent the mole fractions of PEG protons that show fast and slow relaxation, respectively.

Although we do not expect the PEG chains to consist of well-separated segments each with a different T_2, but rather to show a gradient of T_2 times from the point of attachment to the pNIPAm core to the distal end, the experimental relaxation data could be well described by this simplification. This is also shown by the deconvolution of the PEG peak into a broad and a narrow peak (Figure 2b). As expected, the broad peak vanishes after a short relaxation delay τ, whereas the narrow peak decays more slowly. The appearance of a fast relaxing PEG fraction indicates the formation of more rigid, possibly less hydrated, segments[41,42] which we assume to be the parts of the PEG chains that are closest to the micellar cores.[43]

The calculated relaxation times of diblock $mPEG_{2kDa}$-$pNIPAm_{16kDa}$ and triblock $pNIPAm_{16kDa}$-PEG_{4kDa}-$pNIPAm_{16kDa}$ are plotted in Figure 3 (other polymers in Figure S4, Supporting Information). The CP is clearly visible and appears about 1 °C higher in Figure 3 than in Table 1 due to the use of D_2O instead of H_2O.[44] Below the CP, the diblock and triblock show a similar linear relationship of T_1 and T_2 with temperature, with relaxation times that are typical for PEG in aqueous solution.[39,41,45,46] Above the CP, however, there is a small difference in T_1 and a marked difference in T_2. As mentioned, the T_2 decay splits into a fast and slow component both for the diblock and the triblock copolymer. T_{2fast} is longer for the triblock compared to the diblock copolymer micelles (0.09 s vs 0.06 s). This is probably a result of the different hydrodynamic radii of the two micelle types (27 nm vs 35 nm). According to the Stokes−Einstein−Debye relation, this size difference causes the triblock copolymer micelles to have a shorter rotational correlation time than the normal micelles (12 μs vs 27 μs). For the parts of the PEG chains that are directly attached to the micellar core, rotational Brownian motion contributes significantly to T_2 relaxation. Therefore, T_{2fast} is longer for the (faster moving) triblock copolymer micelles.[47] On the other hand, the T_{2slow} of the triblock copolymer is markedly shorter than the T_{2slow} of the diblock. As mentioned, we assume that T_{2slow} describes the relaxation of the distal parts of the PEG chains. The T_2 relaxation of these parts is reduced due to their high flexibility which leads to fast internal motions. Therefore, the observed difference indicates

dx.doi.org/10.1021/la2019605 |Langmuir 2011, 27, 9843–9848

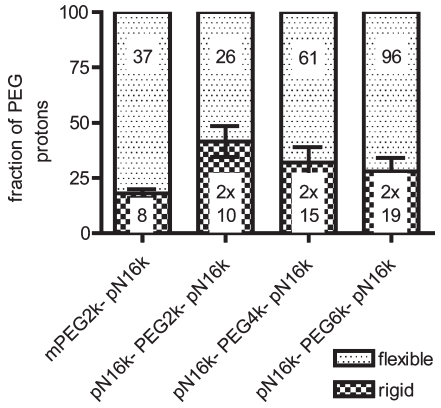

Figure 4. Vertical axis: relative mole fractions of rigid and flexible PEG chain segments for one diblock copolymer and three triblock copolymers measured at 41 °C. The numbers in the bars represent the length (in EO units) of these segments. Error bars represent the 95% confidence interval.

that the flexible distal part of PEG is less flexible in the flowerlike micelles formed by the triblock copolymer than in the starlike micelles formed by the diblock, caused by the formation of strained PEG loops in the former.

The relative contributions of PEG H atoms with fast and slow T_2 relaxation times, f_{fast} and f_{slow}, of the different block copolymers are shown in Figure 4. If the $pNIPAm_{16kDa}$-PEG_{4kDa}-$pNIPAm_{16kDa}$ triblock would behave as a double diblock, the same ratio between rigid and flexible chain segments would be expected as for the $mPEG_{2kDa}$-$pNIPAm_{16kDa}$ polymer.

However, all triblock copolymers clearly have a larger "rigid" fraction than the diblock copolymer. It is calculated that the diblock has one rigid segment of on average eight ethylene oxide (EO) units (18% of 45 units in total), whereas e.g. the $PEG_{4\ kDa}$ triblock has two rigid segments of 15 EO units each (Figure 4). As expected, the relative amounts of flexible segments increase with increasing PEG length, although the absolute size of the rigid segments also increases slightly.

Taken together, these findings indicate that the PEG chains in the corona of the micelles can be regarded as having two parts: a rigid part that is directly attached to the micellar core, which has a fast T_2 decay, and a more flexible distal part, which has a slower T_2 decay.[46] In the flowerlike micelles the rigid part is larger and even the flexible part has a shorter T_2 than in the normal micelles (Figure 3), indicating that the PEG block in the flowerlike micelles is strained above the CP.

CONCLUSION

This work shows that the combination of NMR relaxometry and SLS provides a powerful way to probe the flowerlike conformation of triblock copolymer micelles experimentally. SLS indicated a major structural influence of the looping of the hydrophilic PEG block, whereas ^{1}H NMR T_2 relaxometry could be used to visualize the strain that this looping introduces into the PEG blocks. These data present a direct proof that flowerlike micelles exist and that they are distinctly different from starlike micelles.

ASSOCIATED CONTENT

Supporting Information. Experimental details, characterization, and representative NMR relaxation data. This material is available free of charge via the Internet at http://pubs.acs.org.

AUTHOR INFORMATION

Corresponding Author

*E-mail: W.E.Hennink@uu.nl.

Author Contributions

⊥These authors contributed equally.

ACKNOWLEDGMENT

The authors thank the SONNMRLSF in Utrecht, The Netherlands, for the use of a Bruker 500 MHz NMR spectrometer.

REFERENCES

(1) Torchilin, V. P. *Cell. Mol. Life Sci.* **2004**, *61*, 2549–2559.
(2) Hu, X.; Jing, X. *Expert Opin. Drug Delivery* **2009**, *6*, 1079–1090.
(3) Kumar, N.; Ravikumar, M. N.; Domb, A. J. *Adv. Drug Delivery Rev.* **2001**, *53*, 23–44.
(4) Talelli, M.; Rijcken, C. J.; van Nostrum, C. F.; Storm, G.; Hennink, W. E. *Adv. Drug Delivery Rev.* **2010**, *62*, 231–239.
(5) Chiappetta, D. A.; Sosnik, A. *Eur. J. Pharm. Biopharm.* **2007**, *66*, 303–317.
(6) O'Reilly, R. K.; Hawker, C. J.; Wooley, K. L. *Chem. Soc. Rev.* **2006**, *35*, 1068–1083.
(7) Read, E. S.; Armes, S. P. *Chem. Commun.* **2007**, *29*, 3021–3035.
(8) Oerlemans, C.; Bult, W.; Bos, M.; Storm, G.; Nijsen, J. F.; Hennink, W. E. *Pharm. Res.* **2010**, *27*, 2569–2589.
(9) Torchilin, V. P. *Pharm. Res.* **2007**, *24*, 1–16.
(10) Maeda, H.; Wu, J.; Sawa, T.; Matsumura, Y.; Hori, K. *J. Controlled Release* **2000**, *65*, 271–284.
(11) Owens, D. E.; Peppas, N. A. *Int. J. Pharm.* **2006**, *307*, 93–102.
(12) Zhou, Z.; Chu, B. *Macromolecules* **1994**, *27*, 2025–2033.
(13) Chang, G.; Li, C.; Lu, W.; Ding, J. *Macromol. Biosci.* **2010**, *10*, 1248–1256.
(14) Honda, S.; Yamamoto, T.; Tezuka, Y. *J. Am. Chem. Soc.* **2010**, *132*, 10251–10253.
(15) Hua, S.-H.; Li, Y.-Y.; Liu, Y.; Xiao, W.; Li, C.; Huang, F.-W.; Zhang, X.-Z.; Zhuo, R.-X. *Macromol. Rapid Commun.* **2010**, *31*, 81–86.
(16) Lee, E. S.; Oh, K. T.; Kim, D.; Youn, Y. S.; Bae, Y. H. *J. Controlled Release* **2007**, *123*, 19–26.
(17) Gourier, C.; Beaudoin, E.; Duval, M.; Sarazin, D.; Maitre, S.; Francois, J. *J. Colloid Interface Sci.* **2000**, *230*, 41–52.
(18) Creutz, S.; van Stam, J.; De Schryver, F. C.; Jerome, R. *Macromolecules* **1998**, *31*, 681–689.
(19) Xie, Z.; Lu, T.; Chen, X.; Lu, C.; Zheng, Y.; Jing, X. *J. Appl. Polym. Sci.* **2007**, *105*, 2271–2279.
(20) Balsara, N. P.; Tirrell, M.; Lodge, T. P. *Macromolecules* **1991**, *24*, 1975–1986.
(21) Linse, P. *Macromolecules* **1993**, *26*, 4437–4449.
(22) Sprakel, J.; Besseling, N. A.M.; Leermakers, F. A.M.; Cohen Stuart, M. A. *J. Phys. Chem. B* **2007**, *111*, 2903–2909.
(23) Giacomelli, F. C.; Riegel, I. C.; Petzhold, C. L.; da Silveira, N. P.; Stepanek, P. *Langmuir* **2009**, *25*, 3487–3493.
(24) Giacomelli, F. C.; Riegel, I. C.; Petzhold, C. L.; da Silveira, N. P.; Stepanek, P. *Langmuir* **2009**, *25*, 731–738.
(25) Rodrigues, K.; Mattice, W. L. *Langmuir* **1992**, *8*, 456–459.
(26) Rodrigues, K.; Mattice, W. L. *Polym. Bull.* **1991**, *2*, 239–243.
(27) Schild, H. G. *Prog. Polym. Sci.* **1992**, *17*, 163–249.
(28) Ciampolini, M.; Nardi, N. *Inorg. Chem.* **1966**, *5*, 41–44.
(29) Neradovic, D.; Soga, O.; Van Nostrum, C. F.; Hennink, W. E. *Biomaterials* **2004**, *25*, 2409–2418.
(30) Wilhelm, M.; Zhao, C. L.; Wang, Y.; Xu, R.; Winnik, M. A.; Mura, J. L.; Riess, G.; Croucher, M. D. *Macromolecules* **1991**, *24*, 1033–1040.
(31) Teodorescu, M.; Negru, I.; Stanescu, P. O.; Drăghici, C.; Lungu, A.; Sârbu, A. *React. Funct. Polym.* **2010**, *70*, 790–797.

(32) Xia, Y.; Yin, X.; Burke, N. A. D.; Stöver, H. D. H. *Macromolecules* **2005**, *38*, 5937–5943.
(33) Topp, M. D. C.; Dijkstra, P. J.; Talsma, H.; Feijen, J. *Macromolecules* **1997**, *30*, 8518–8520.
(34) Van Butsele, K.; Cajot, S.; Van Vlierberghe, S.; Dubruel, P.; Passirani, C.; Benoit, J.; Jérôme, R.; Jérôme, C. *Adv. Funct. Mater.* **2009**, *19*, 1416–1425.
(35) Liu, T.; Kim, K.; Hsiao, B. S.; Chu, B. *Polymer* **2004**, *45*, 7989–7993.
(36) Aharoni, S. M.; Murthy, N. S. *Polym. Commun.* **1983**, *24*, 132.
(37) Walderhaug, H.; Söderman, O. *Curr. Opin. Colloid Interface Sci.* **2009**, *14*, 171–177.
(38) Convertine, A. J.; Lokitz, B. S.; Vasileva, Y.; Myrick, L. J.; Scales, C. W.; Lowe, A. B.; McCormick, C. L. *Macromolecules* **2006**, *39*, 1724–1730.
(39) Cau, F.; Lacelle, S. *Macromolecules* **1996**, *29*, 170–178.
(40) Poe, G. D.; Jarrett, W. L.; Scales, C. W.; McCormick, C. L. *Macromolecules* **2004**, *37*, 2603–2612.
(41) Bedu-Addo, F. K.; Tang, P.; Xu, Y.; Huang, L. *Pharm. Res.* **1996**, *13*, 710–717.
(42) Lüsse, S.; Arnold, K. *Macromolecules* **1996**, *29*, 4251–4257.
(43) Valentini, M.; Napoli, A.; Tirelli, N.; Hubbell, J. A. *Langmuir* **2003**, *19*, 4852–4855.
(44) Ma, J.; Guo, C.; Tang, Y.; Xiang, J.; Chen, S.; Wang, J.; Liu, H. *J. Colloid Interface Sci.* **2007**, *312*, 390–396.
(45) Heald, C. R.; Stolnik, S.; Kujawinski, K. S.; De Matteis, C.; Garnett, M. C.; Illum, L.; Davis, S. S.; Purkiss, S. C.; Barlow, R. J.; Gellert, P. R. *Langmuir* **2002**, *18*, 3669–3675.
(46) Garcia-Fuentes, M.; Torres, D.; Martín-Pastor, M.; Alonso, M. J. *Langmuir* **2004**, *20*, 8839–8845.
(47) Törnblom, M.; Henriksson, U.; Ginley, M. *J. Phys. Chem.* **1994**, *98*, 7041–7051.